JOURNAL OF COMPUTATIONAL PHYSICS 64, 368–379 (1986)

On Vector Potential–Vorticity Methods for Incompressible Flow Problems

O. R. TUTTY

Department of Applied Mathematics and Theoretical Physics, University of Cambridge, Silver Street, Cambridge CB3 9EW, England

Received December 6, 1984; revised July 8, 1985

The vector and scalar potential formulation for three-dimensional laminar incompressible flow is examined. In problems with through-flow, it is shown that the scalar potential can introduce a spurious discontinuity into the boundary conditions. The result is unacceptable numerical errors. This is illustrated using, for simplicity, two-dimensional Stokes flows. Alternative vector potential–vorticity formulations which eliminate this difficulty are considered.

1. INTRODUCTION

To date, nearly all numerical three-dimensional incompressible flow calculations have used the primitive variables, i.e., have calculated the velocity and pressure directly, while the most popular approach for two-dimensional calculations is the streamfunction–vorticity formulation. The streamfunction has the important advantage that continuity is explicitly satisfied both globally and locally, whereas local continuity is implicit only using most pressure–velocity methods. Problems with continuity can arise when calculating the velocity directly. For example, the velocity–vorticity formulation of Dennis, Ingham, and Cook [1] encounters severe difficulties near a corner singularity (Tutty [2]).

The vector potential–vorticity and scalar and vector potential–vorticity formulations are three-dimensional analogues of the streamfunction–vorticity method, and enforce local as well as global continuity. They have not been widely used because of their increased storage and computational requirements and, until recently, uncertainty about suitable boundary conditions. Hirasaki and Hellums [3] were the first to present general boundary conditions for the vector potential. Their conditions are simple for flows with impermeable boundaries, but require the solution of partial differential equations on boundaries with through-flow. Hirasaki and Hellums [4] and Richardson and Cornish [5] introduce a scalar potential to the formulation, which simplifies the conditions for through-flow at the expense of a further variable.

Unfortunately the scalar potential can introduce numerical errors near a sharp corner with through-flow, since, in general, there will be a discontinuity in its boun-

0021-9991/86 $3.00

dary conditions at such a corner. With a finite-difference scheme, this discontinuity has an effect similar to that of resolving a Gibbs phenomenon with a finite number of Fourier components, and leads to nonphysical variations in the calculated values near the corner. Wong and Reizes [6] found such behaviour when calculating three-dimensional duct flows.

In this paper, a number of scalar and vector potential formulations are considered, and the effects of the discontinuity in the boundary conditions are demonstrated using, for simplicity, two-dimensional Stokes problems. In Section 2 the equations are presented, Section 3 details the problems arising from the scalar potential, Section 4 presents alternative formulations, and the conclusions can be found in Section 5.

Throughout this paper, unless specifically mentioned, standard central difference formulae and a square grid with $h = 1/16$ are used in numerical calculations.

2. The Stokes Equations

The Stokes equations, which govern the slow flow of a viscous incompressible fluid, are

$$\nabla \cdot \mathbf{u} = 0, \tag{2.1}$$

$$\nabla^2 \mathbf{u} = \nabla p, \tag{2.2}$$

where $\mathbf{u} = (u, v, w)$ and p are the velocity vector and pressure. Taking the curl of (2.2) produces the vorticity transport equation

$$\nabla^2 \boldsymbol{\zeta} = 0 \tag{2.3}$$

where

$$\boldsymbol{\zeta} = \nabla \times \mathbf{u} \tag{2.4}$$

is the vorticity vector. Using Helmholtz's theorem, the velocity vector can be expressed in terms of a scalar potential ϕ and a vector potential $\boldsymbol{\psi}$ as

$$\mathbf{u} = \nabla \phi + \nabla \times \boldsymbol{\psi}. \tag{2.5}$$

Without loss of generality, $\boldsymbol{\psi}$ can be made solenoidal, i.e.,

$$\nabla \cdot \boldsymbol{\psi} = 0. \tag{2.6}$$

Moreover, since $\mathbf{u}$ is itself solenoidal, ϕ can be set identically zero while (2.6) will still hold. Substituting (2.5) in (2.1) gives

$$\nabla^2 \phi = 0, \tag{2.7}$$

while taking the curl of (2.5) and using (2.6) yields

$$\nabla^2\psi = -\zeta. \tag{2.8}$$

The boundary conditions for the potentials, from Hirasaki and Hellums [3] and Richardson and Cornish [5], are

$$\frac{\partial\phi}{\partial n} = h_n u_n \tag{2.9}$$

and

$$\psi_t = \psi_\tau = \frac{\partial}{\partial n}(h_t h_\tau \psi_n) = 0 \tag{2.10}$$

if the region is simply connected, where n, t, and τ denote the normal and tangential components, and h_n, h_t, and h_τ are the appropriate scale factors.

Only the normal component of velocity is used in the boundary conditions given above. The other two components will in general be used in calculating the tangential vorticity on the boundary, for which either local (e.g., Mallinson and de Vahl Davis [7], Wong and Reizes [6]) or global (Quartapelle and Valz-Gris [8], Glowinski and Pironneau [9]) methods are available.

3. Difficulties Associated with the Scalar Potential

Consider a right-angled corner formed by $x \geqslant 0$ and $y \geqslant 0$ with velocities $u_b(y)$ and $v_b(x)$ across $x = 0$ and $y = 0$, respectively, where (x, y, z) are cartesian coordinates. From (2.9)

$$\frac{\partial\phi}{\partial x} = u_b \quad \text{on} \quad x = 0 \qquad \text{and} \qquad \frac{\partial\phi}{\partial y} = v_b \quad \text{on} \quad y = 0.$$

Hence, unless

$$\operatorname*{Limit}_{l \to 0^+} \left\{ \frac{\partial u_b}{\partial y}(l) - \frac{\partial v_b}{\partial x}(l) \right\} = 0, \tag{3.1}$$

the use of (2.9) will introduce a discontinuity into the problem for ϕ. This discontinuity may be spurious in the sense that it can arise with continuous, and indeed regular, flow fields (e.g., Poiseuille flow—see below). Clearly (3.1) will not be true in general. A condition similar to (3.1) must hold on any sharp corner if (2.9) is to be continuous. Note that (3.1) may be satisfied by boundary velocities that are discontinuous at $x = y = 0$, and that it does not necessarily imply $\zeta_z = 0$ at $x = y = 0$, as will be seen below.

Equation (3.1) requires the existence of the mixed derivative $\partial^2\phi/\partial x\,\partial y$ at the corner point, and is a stronger condition than is formally required for the solution of the Neumann problem formed by (2.7) and (2.9). However, in the absence of a condition similar to (3.1), a numerical solution is unlikely to provide accurate values for ϕ for the points near the corner. Moreover, as will be shown below, unless a very fine grid is used near the corner, the violation of (3.1) can result in unacceptable errors near the corner even with an accurate solution for ϕ.

To illustrate the numerical effect of this discontinuity, several simple two-dimensional flows in the $x-y$ plane will be considered: first, Poiseuille flow on a unit square, i.e., $\mathbf{u}=(U_0(y), 0)$ where $U_0=y(1-y)$. The scalar potential, ϕ, $\psi=\psi_z$, and $\zeta=\zeta_z$ are nonzero. A numerical solution was found with the square grid $x_i=ih$, $y_j=jh$; $i, j=0, 1,..., N$. All finite-difference equations in the interior of the region are obvious. For the boundary vorticity, Eqs. (2.5) and (2.8) produce, for example,

$$\zeta_{i,0}=-[2\psi_{i,1}+\phi_{i+1,0}-\phi_{i-1,0}]/h^2, \qquad i=1, 2,..., N-1 \tag{3.2}$$

on $y=0$, where $\psi_{i,j}=\psi(x_i, y_j)$, etc. More complex formulae, such as those given by Wong and Reizes [6], could be used, but would not qualitatively affect the results presented in this paper. Note that, strictly, Helmholtz's theorem (2.5) applies only in the interior of the region and not on the boundary. However, (3.2) can be obtained using (2.4) and (2.5) in the fluid near the boundary and taking the correct limit. In contrast, (2.5) and (2.8) do not in general give valid formulae at the corners. For example, (2.8) and $\partial\psi/\partial x=\partial\psi/\partial y=0$ (from $u=v=0$ at $(0, 0)$) yield

$$\zeta_{0,0}=-2[\psi_{1,0}+\psi_{0,1}-2\psi_{0,0}]/h^2 \tag{3.3a}$$

which, with $\psi=0$ on the boundaries, produces $\zeta=0$ at $(0, 0)$. If instead the vorticity at $(0, 0)$ is defined as

$$\zeta=\operatorname*{Limit}_{l\to 0^+}\left\{\frac{\partial v}{\partial x}(l, 0)-\frac{\partial u}{\partial y}(0, l)\right\}$$

then

$$\zeta_{0,0}=\lim_{l\to 0^+}\left\{\frac{\partial^2\phi}{\partial x\partial y}(l, 0)-\frac{\partial^2\phi}{\partial x\,\partial y}(0, l)\right\} \tag{3.3b}$$

is obtained, where again $\psi=0$ on the boundaries has been used. For the present problem with Poiseuille flow, (3.3b) reduces to

$$\zeta_{0,0}=-U_0^1(0),$$

which is the correct value.

In a manner similar to that used to obtain (3.2), (2.7) and (2.9) yield finite-difference equations for the boundary values of ϕ. Alternatively, one-sided $O(h^2)$

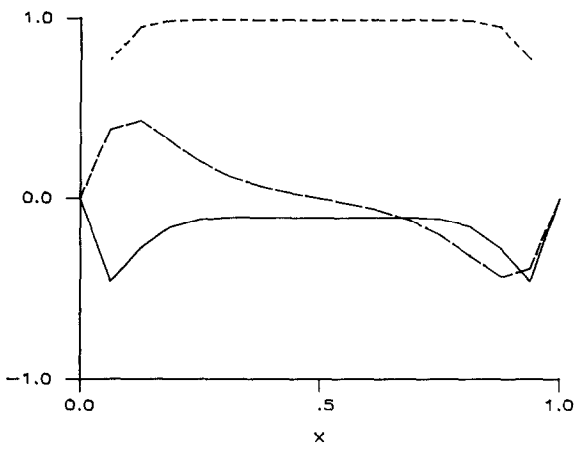

FIG. 1. Velocity and wall shear for Poiseuille flow $\phi - \psi - \zeta$ problem. Solid line: $(u - U_0(y)) \times 200$, $y = h = 1/16$; long dashed line: $v \times 200$, $y = h = 1/16$; short dashed line: $\partial u/\partial y$ $(= -\zeta)$ at $y = 0$, $h = 1/16$.

differencing could be used with (2.9) alone. Both these methods were tried, with similar results. All results presented below use the former method.

Figure 1 gives the velocity near the wall and the wall shear. Near the corners, there is an unreasonable variation in these results, with the wall shear showing a marked decrease. Wong and Reizes [6] argued that these unacceptable results are due to a failure of the velocity from the scalar potential to satisfy locally a difference form of the continuity equation. This argument appears to be in direct conflict with a basic strength of the scalar and vector potential method, i.e., that the continuity equation—(2.7)—is satisfied identically at every point in the grid. Wong and Reizes considered a cell with sides a distance h (i.e., one grid step) away from the centre point, and found that the net flow into this cell is small but not, in general, zero. Instead, consider a cell with sides a distance $h/2$ from the centre point. Calculating the velocity at the midpoints of the cell walls and substituting in the finite-difference form of (2.1) gives

$$[\phi_{i+1,j} + \phi_{i-1,j} + \phi_{i,j+1} + \phi_{i,j-1} - 4\phi_{i,j}]/h^2 = 0 \tag{3.4}$$

which is the standard finite-difference form of (2.7). Hence the continuity equation (2.1) is satisfied locally as well as globally by the potential flow given by ϕ. Simple arithmetic means—a process which is $O(h^2)$ accurate—can be used to obtain values of ψ at the corners of the (later) cell, and the velocity so obtained at the midpoints of the cell walls satisfies the difference form of (2.1) identically. Therefore the velocity distribution obtained from (2.5) satisfies continuity locally as well as globally.

It is interesting to consider the analytic solution for ϕ for this problem.

$$\phi = a_0 x + \sum_{n=1}^{\infty} [a_n e^{n\pi x} + b_n e^{-n\pi x}] \cos(n\pi y) \tag{3.5}$$

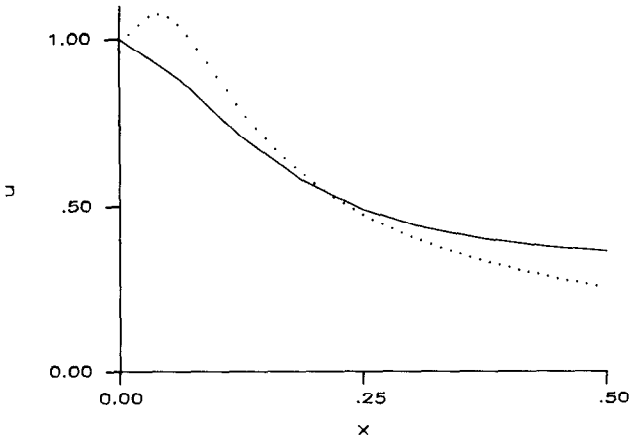

FIG. 2. Axial velocity u for entry flow ($y = h = 1/16$). Solid line: from the $\psi - \zeta$ problem with (4.1) and (4.3); dotted line: from the Stokes expansion (4.5).

satisfies (2.7) and (2.9) on $y = 0$ and 1. The solution is completed by (2.9) at $x = 0$ and 1 and the cosine series for $U_0(y)$. However, to obtain accurate values from (3.5), enough terms must be used to resolve the Gibbs phenomenon arising from the discontinuity of the derivative at the corners. Numerically this is equivalent to using sufficient points in y.

The calculation for ψ and ζ was repeated using highly accurate values of ϕ obtained from (3.5). There was no significant improvement in the results. In particular, the wall shear was close to that shown in Fig. 1. Hence, obtaining accurate values for ϕ is not sufficient to ensure an accurate solution for the basic flow problem.

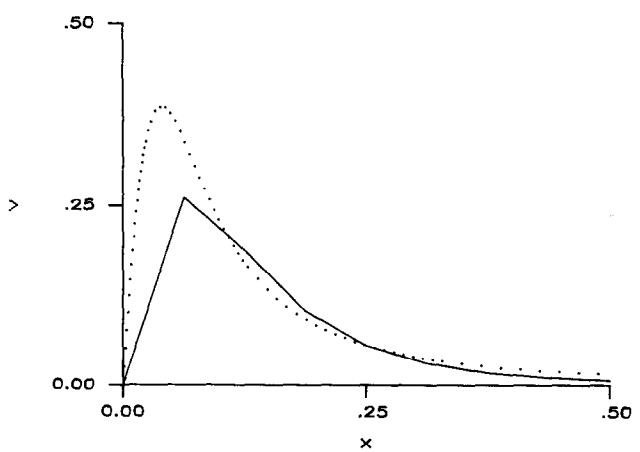

FIG. 3. Transverse velocity v for entry flow ($y = h = 1/16$). Solid line: from the $\psi - \zeta$ problem with (4.1) and (4.3); dotted line: from the Stokes expansion (4.6).

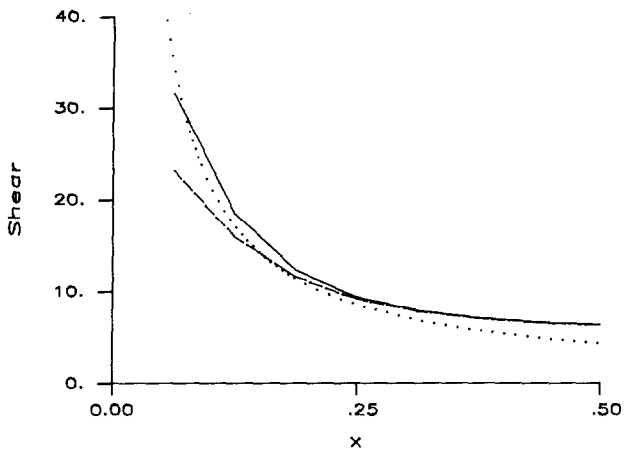

FIG. 4. Wall shear for entry flow ($y=0$, $h=1/16$). Solid line: from the $\psi-\zeta$ problem with (4.1) and (4.3); dashed line: from the $\phi-\psi-\zeta$ problem with (3.2); dotted line: from the Stokes expansion (4.8).

A second problem is that of entry flow into a channel of width one (the two-dimensional Stokes version of the duct flow problem considered by Aregbesola and Burley [10] and Wong and Reizes [6]). If the entry profile is uniform with zero transverse velocity (i.e., $\mathbf{u}=(1,0)$ at $x=0$), then (3.1) is satisfied and the scalar–vector potential method might be expected to give good results at the inlet, but poor results near the walls at the outlet if Poiseuille flow ($6U_0(y)$) is assumed there. First, however, there is another difficulty in calculating the scalar potential for this problem. Equations (2.7) and (2.9) provide one difference equation for each grid point, but this system is not independent (if it were it would violate the non-uniqueness of the Neumann problem). Moreover, an independent system of finite-

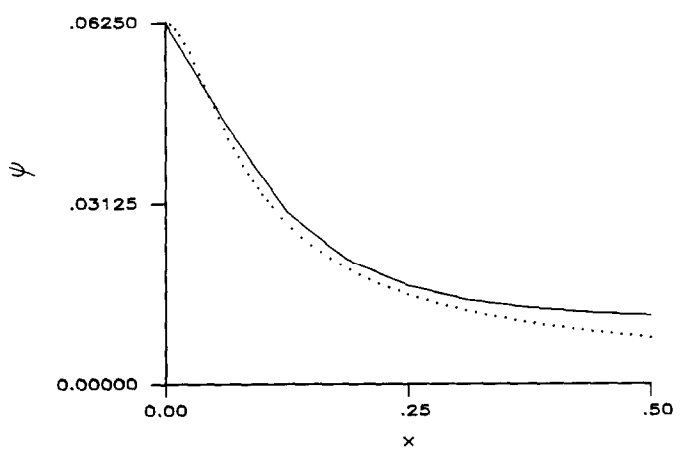

FIG. 5. Streamfunction for entry flow ($y=h=1/16$). Solid line: from the $\psi-\zeta$ problem with (4.1) and (4.3); dotted line: from the Stokes expansion (4.4).

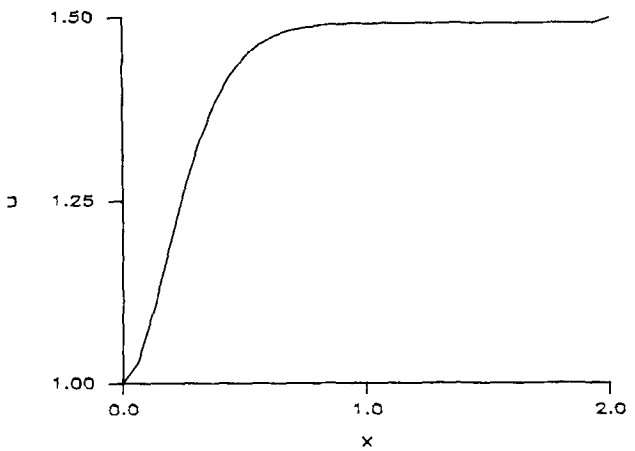

FIG. 6. Centre line velocity u ($y = 1/2$, $h = 1/16$). Solid line: from the $\psi - \zeta$ problem with (4.1) and (4.3).

difference equations may not be consistent with the prescribed boundary conditions, except in a limiting sense. For example, for a cuboid or rectangle with a rectangular grid, suppose that (2.7) is used at each interior point and (2.7) and (2.9) at all except one boundary point, with standard $O(h^2)$ central differences used in the interior and formulae similar to (3.2) on the boundaries. Then it can be shown that the velocity implied at the other boundary point is such that trapezoidal rule integration over the surface will give zero net flow into the region. In particular, with the entry flow, suppose that $\phi_{0,0}$ is fixed, and that $\mathbf{u} = (1, 0)$ at $(0, 1)$. The trapezoidal rule has a nonzero error for Poiseuille flow, hence the numerical solution will not have $\mathbf{u} = (1, 0)$ at $(0, 0)$, and will not be symmetric. If symmetry is used explicitly the implied velocity at $(0, 0)$ will not give a uniform inlet profile. Note (i) the velocity tends to uniform as the step length decreases and (ii) a slip velocity at the wall (or a suitable scaling of the velocity at the outlet) could be used to force $\mathbf{u} = (1, 0)$ at $(0, 0)$.

Calculations were performed (with a slip velocity) for a channel with $x_{\max} = 2$, which allowed the flow to develop fully. As expected, there is a kink in the results near the outlet similar to that for the Poiseuille flow. Figures 2–5 show various results near the inlet. The wall shear appears (as would be hoped) to be singular as $x \to 0+$ (Fig. 4). By using both $\partial\phi/\partial x = 1$ and $u = 0$ at $(0, 0)$, the difference form of (2.8) yields $\zeta_{0,0} = -2/h$, which is consistent with the calculated values for the wall shear. Note that (2.8) can be used here as $\partial^2\phi/\partial x\,\partial y$ exists at the corner.

4. ALTERNATIVE FORMULATIONS

Since the difficulties described in Section 3 arise from the scalar potential, it would be useful to eliminate it from the problem. This should also have storage and

computational advantages. Hirasaki and Hellums [3] use only the vector potential, but on each boundary with through-flow they require the solution of a partial differential equation to determine the conditions on ψ. If the velocity normal to the boundaries is known a priori, these equations could be solved independently of the internal calculation. For two-dimensional problems, this formulation reduces to the "standard", streamfunction–vorticity problem.

Fortunately the conditions can be simplified on at least some of the boundaries by a straightforward modification of the Hirasaki and Hellums [3] formulation. Instead of (2.5), let $\mathbf{u}$ be

$$\mathbf{u} = \mathbf{u}_s + \nabla \times \boldsymbol{\psi}, \tag{4.1}$$

where $\mathbf{u}_s$ is necessarily solenoidal. Also, without loss of generality, let $\boldsymbol{\psi}$ be solenoidal. Taking the curl of (4.1) and using (2.6) gives

$$\nabla^2 \boldsymbol{\psi} = -\boldsymbol{\zeta} + \nabla \times \mathbf{u}_s \tag{4.2}$$

in place of (2.8). If the normal component of $\mathbf{u}_s$ is the normal velocity on a boundary, (2.10) applies on that boundary. In practice, the choice of $\mathbf{u}_s$ will depend on the problem. For example, for the flow through a cuboid with known normal boundary velocities, (2.10) could be used on *at least* three of the boundaries. Note that a solenoidal vector can be formed on a planar boundary by taking only the velocity normal to the boundary.

Wong and Reizes [6] present a formulation which is similar to the above, but with $\mathbf{u}_s$ irrotational as well as solenoidal. For their duct problem there was an obvious choice for $\mathbf{u}_s$, but, in general, it may not be a simple task to find an appropriate irrotational flow. Further, a potential $\mathbf{u}_s$ that will introduce (2.10) may not give a satisfactory solution, and, in fact, may itself explicitly introduce the discontinuity and the resulting errors. For example, in the Poiseuille flow problem of Section 3, taking $\mathbf{u}_s$ from the divergence of the scalar potential (3.5)—or equivalently performing a $\phi - \psi - \zeta$ calculation with analytic ϕ from (3.5)—does not give accurate values near the corners. In contrast, $\mathbf{u}_s = (U_0 + x^2, -xU_0')$ is irrotational and introduces (2.10) on $x = 0$ (although not on $y = 0$ and 1), and numerically gives the exact solution $\psi = -\frac{1}{2}x^2 U_0'$. However, if the requirement that $\mathbf{u}_s$ be irrotational is dropped, the solution comes out simply as $\mathbf{u}_s = (U_0, 0)$ and $\psi = 0$.

Consider now the entry flow problem of Section 3. The "modified" problem with (4.1) and $\mathbf{u}_s = (1, 0)$ and the standard $\psi - \zeta$ problem produce identical results. As expected, the solution with formulae similar to (3.2) on the boundaries is very close to that with the scalar potential over most of the grid. Near the outlet it is much improved, although there is still an error—less than 1% in the vorticity— due to the $O(h)$ accuracy of (3.2). Woods' [11] $O(h^2)$ formula, e.g.,

$$\zeta_{i,0} = -\frac{1}{2}\zeta_{i,1} + \frac{3}{h^2}(\psi_{i,0} - \psi_{i,1}) \qquad \text{on} \quad y = 0, \tag{4.3}$$

yields the correct solution downstream (to seven significant figures in the streamfunction and five in the vorticity). Figures 2–6 display various results. Except for the wall shear (Fig. 4), the values from the $\phi-\psi-\zeta$ and $\psi-\zeta$ calculations with (3.2) are omitted as, over the range shown, they are graphically identical to the values from $\psi-\zeta$ with (4.3). The major difference between the values with (3.2) and those with (4.3) is in the vorticity near the inlet, (4.3) giving a much sharper rise as $x\to 0+$. Equation (4.3) is valid at (0, 0), and with $\psi_{0,1}=h$ produces $\zeta_{0,0}=-56.2$. Again this is consistent with the calculated values for the wall shear for $x>0$ (Fig. 4). The apparent kink in u for $y=\frac{1}{2}$ near the outlet with the "exact" downstream solution (see Fig. 6) comes from the $O(h^2)$ error in the standard central difference approximation for $\partial/\partial y$, and can be removed by using a more accurate difference formula (e.g., of $O(h^4)$) for $\partial/\partial y$ when calculating u from ψ.

Near the corner, the leading term of the Stokes expansion is

$$\psi = kr\left[\theta\cos\theta+\left(\frac{\pi}{2}\theta-1\right)\sin\theta\right], \tag{4.4}$$

where $k=4/(\pi^2-4)$, (r,θ) are standard polar coordinates with origin $x=y=0$ and $\theta=0$ the positive x-axis, and $r\ll 1$ (Moffatt [12], Gupta, Manohar, and Noble [13]). From (4.4), the cartesian velocity components and the vorticity are

$$u=\frac{1}{2}k\left[\frac{\pi}{2}(2\theta+\sin 2\theta)-1+\cos 2\theta\right], \tag{4.5}$$

$$v=\frac{1}{2}k\left[2\theta-\sin 2\theta-\frac{\pi}{2}(1-\cos 2\theta)\right], \tag{4.6}$$

and

$$\zeta=-\frac{k}{r}\left[\frac{\pi}{2}(2\cos\theta-\sin\theta)-\sin\theta\right], \tag{4.7}$$

TABLE I

Transverse Velocity on $y=h=1/16$ for Entry Flow

				Percentage difference		
x	v_s	v_n	v_d	n/s	d/s	n/d
h	0.3407	0.2606	0.2766	−23.5	−18.8	−5.8
$2h$	0.1707	0.1871	0.1869	9.6	9.5	0.1
$3h$	0.09222	0.1032	0.09910	11.9	7.5	4.1
$4h$	0.05637	0.05577	0.05915	−1.1	4.9	−5.7

Note. v_s is from (4.6), v_n from the numerical solution of $\psi-\zeta$ with (4.3), and v_d is from (4.4) and central differences. n/s denotes $(v_n/v_s-1)\times 100$, etc.

TABLE II

Entry Flow Streamfunction for $y = h = 1/16$

x	ψ_s	ψ_n	% difference
h	0.04341	0.04491	3.4
$2h$	0.02792	0.02993	7.2
$3h$	0.02005	0.02152	7.3
$4h$	0.01554	0.01702	9.5

Note. ψ_s is from (4.4), ψ_n is from the numerical solution of $\psi - \zeta$ with (4.3), and the difference is $(\psi_n/\psi_s - 1) \times 100$.

respectively. Along the lower wall ($\theta = 0$) (4.7) gives

$$\zeta = -k\pi/r. \tag{4.8}$$

Near the corner, the streamfunction and voriticity from the numerical solution have the behaviour predicted by (4.4) and (4.8) (see Figs. 4 and 5), but the velocity shows a large difference (Figs. 2 and 3). Most of this is from the error in the difference formla used to calculate the velocities, as can be seen from Table I (u shows a similar pattern). For comparison, Table II gives values of ψ.

The numerical solutions were calculated using an ADI method. Convergence was extremely slow for ϕ because of the derivative boundary conditions. For the entry problem, ϕ needed approximately 10,700 complete sweeps to converge (i.e., for the sum of the changes to be less than 10^{-6} in a single sweep), while the $\psi - \zeta$ part of the problem converged in 122 complete sweeps. Thus nearly all the computational effort was in finding ϕ. With (3.2), the standard and modified problems took 137 and 122 complete sweeps respectively. This is approximately 1/40th of the computational effort required for the $\phi - \psi - \zeta$ problem. With the Woods formula, 278 and 265 sweeps were needed for the standard and modified $\psi - \zeta$ problems. No attempt was made to optimize the rate of convergence.

5. Conclusions

The discontinuity in the boundary conditions for the scalar potential which can occur at a sharp corner may have an unacceptable effect on numerical calculations. This has been illustrated using simple two-dimensional Stokes flows. It is stressed that these effects will occur in more complex three-dimensional flows, including steady and unsteady Navier–Stokes calculations. Indeed, they were first observed by the present author in a three-dimensional study, the results of which will be published elsewhere.

Concerning the discontinuity:

(i) it is local in effect;

(ii) it is grid dependent, and its effect will be reduced but not eliminated by decreasing the grid step;

(iii) continuous boundary conditions can be achieved when there is a discontinuity in the flow, and the scalar potential might be of use in such problems;

(iv) using an analytic or an accurate numerical scalar potential/potential velocity will not necessarily produce an accurate solution.

If the scalar potential is dropped from the problem, Hirasaki and Hellums [3] give a general formulation, for which (4.1) provides a useful simplification. Although this formulation may require the solution of partial differential equations on the boundaries, it is possible that the end result will be less computational effort, because of the slow convergence of the Neumann problem for the scalar potential.

Finally, if an accurate vector potential is found numerically, the standard central difference formula may not give sufficiently accurate values for the velocity. This might have serious consequences in Navier–Stokes calculations where the velocity is explicitly required in the vorticity transport equations.

ACKNOWLEDGMENTS

This research was funded by SERC, U. K., and NSERC, Canada, and was carried out in part at the University of Western Ontario, London, Canada. The referees are thanked for their helpful comments on the manuscript.

REFERENCES

1. S. C. R. DENNIS, D. B. INGHAM, AND R. N. COOK, *J. Comput. Phys.* **33**, p. 325 (1979).
2. O. R. TUTTY, submitted for publication.
3. G. J. HIRASAKI AND J. D. HELLUMS, *Quart. Appl. Math.* **26**, p. 331 (1968).
4. G. J. HIRASAKI AND J. D. HELLUMS, *Quart. Appl. Math.* **28**, p. 293 (1970).
5. S. M. RICHARDSON AND A. R. H. CORNISH, *J. Fluid Mech.* **82**, p. 309 (1977).
6. A. K. WONG AND J. A. REIZES, *J. Comput. Phys.* **55**, p. 98 (1984).
7. G. D. MALLINSON AND G. DE VAHL DAVIS, *J. Comput. Phys.* **12**, p. 435 (1973).
8. L. QUARTAPELLE AND F. VALZ-GRIS, *Int. J. Numer. Methods Fluids* **1**, p. 129 (1981).
9. R. GLOWINSKI AND O. PIRONNEAU, *SIAM Rev.* **12**, p. 167 (1979).
10. Y. A. S. AREGBESOLA AND D. M. BURLEY, *J. Comput. Phys.* **24**, p. 398 (1977).
11. L. C. WOODS, *Aero. Quart.* **5** p. 176 (1954).
12. H. K. MOFFATT, *J. Fluid. Mech.* **18**, p. 1 (1964).
13. M. M. GUPTA, R. P. MANOHAR, AND B. NOBLE, *Comput. & Fluids* **9**, p. 379 (1981).